RESEARCH PAPER

Effect of thermal treatments on sputtered silver nanocluster/silica composite coatings on soda-lime glasses: ionic exchange and antibacterial activity

M. Ferraris · S. Ferraris · M. Miola · S. Perero ·
C. Balagna · E. Vernè · G. Gautier · Ch. Manfredotti ·
A. Battiato · E. Vittone · G. Speranza · I. Bogdanovic

Abstract Silver nanocluster/silica composite coatings were deposited on both soda-lime and silica glasses by radio frequency (RF) co-sputtering. The effect of thermal treatments on the microstructure in the range of 150–450 °C were examined by UV–visible spectroscopy, X-ray diffraction, X-ray photoelectron spectroscopy and Time of Flight-Elastic Recoil Detection Analysis. Sodium/silver ionic exchange was evidenced for coatings sputtered on soda-lime substrates after heating at 450 °C; presence of silver ions and/or silver nanoclusters, nanocluster size and their position inside the sputtered layers will be discussed for as-deposited and heated coatings on both substrates. The antibacterial activity of all coatings was determined against *Staphylococcus aureus* and *Candida albicans* by disk diffusion method and colonies forming units count; in agreement with microstructural results, the antibacterial activity present on all coatings was slightly reduced after heating at 450 °C. All coatings have been submitted to humidity plus UV ageing and sterilization by autoclave, gamma ray and ethylene oxide gas. Tape resistance (ASTM D3359-97) tests have been done on each coating before and after ageing and sterilizations, revealing a good adhesion on soda-lime substrates, except for those aged in humidity plus UV and sterilized by autoclave. Scratch tests and nanoindentation tests have been done on each coating, as-deposited and after heating at 450 °C. The coating hardness was improved by heating only when coatings were deposited on silica. The heating of coatings deposited on soda-lime substrates gave opposite effect on their hardness.

Keywords Antibacterial · Sputtering · Silver nanoclusters · Ionic exchange · Soda-lime

M. Ferraris · S. Ferraris (✉) · M. Miola ·
S. Perero · C. Balagna · E. Vernè
Department of Applied Science and Technology, Institute of Materials Physics and Engineering, Politecnico di Torino, Turin, Italy
e-mail: sara.ferraris@polito.it

G. Gautier
IMAMOTER Institute for Agricultural and Earthmoving Machines, Turin, Italy

Ch. Manfredotti · A. Battiato · E. Vittone
Physics Department, NIS Excellence Centre and CNISM, University of Torino, Turin, Italy

G. Speranza
Fondazione Bruno Kessler FBK, Trento, Italy

I. Bogdanovic
Experimental Physics Department, Ruđer Bošković Institute, Zagreb, Croatia

Introduction

Several coatings showing antibacterial effect are more and more subject of scientific investigation (and market interest) not only for biomedical implants (Chen et al. 2006), but also to coat various materials

🖄 Springer

such as yarns, fabrics, glass, and other substrates to be used in everyday life (Tunc and Olgun 2006; Martin et al. 2007; Kim et al. 2007; Verné et al. 2005).

Metallic silver, with its long-term history of antibacterial agent, is the most widely used metal for these coatings. Its main advantage is the wide spectrum of antibacterial activity, the low development of resistance compared to antibiotics and ability to inhibit polymicrobial/fungal colonization (Kramer et al. 1981).

Although there is still some debate on the mechanism, silver antibacterial properties are mostly due to the release of ionic silver and/or to the presence of silver nanoclusters, which interfere with a wide range of biochemical processes resulting in a range of effects from inhibition of growth, loss of infectivity to cytotoxicity (Rai et al. 2009; Castellano et al. 2007; Landsdown 2002; Sondi and Salopek-Sondi 2004; Morones et al. 2005).

Since pure metallic silver has a relatively low mechanical and chemical stability, silver is usually embedded in polymers or zeolites to obtain antibacterial coatings (http://www.agion-tech.com/, Kim et al. 2008; Brook et al. 2007; Masuda et al. 2007, US Pat No 7,232,777); however, the main drawback of the available polymer-based antibacterial coatings is that they generally do not have a high mechanical and thermal stability and their life-time is limited.

Ionic exchange is a well-known method to obtain stable silver ion rich surfaces on sodium- or potassium-containing glasses (Najafi 1992), such as soda-lime glasses, which are the most common and widely used glasses for a huge number of applications, window glasses, Automatic Teller Machines (ATMs), computers, cell phones and electronic book readers touch screen, just to cite few of them.

Recently, antibacterial functionality for soda-lime glasses obtained by silver/sodium ionic-exchange has attracted the attention of researchers (Durucan and Akkopru 2010; Di Nunzio et al. 2004; Verné et al. 2009) and companies. In particular because silver ion exchanged soda-lime glasses have both improved mechanical strength and antibacterial effect (Borrelli et al. 2012, http://www.agc-flatglass.sg/products-detail.aspx?id=32).

However, ionic exchange is intrinsically limited to glasses containing exchangeable ions such as sodium and potassium ions. Another method to obtain stable and thermo-mechanically reliable silver rich surfaces is to deposit silver-doped silica thin films. They can be sputtered (Ferraris et al. 2008, 2010a, b, 2011; Balagna et al. 2012; Sangpour et al. 2009; Jimenez et al. 2011) or deposited by sol–gel on different substrates, not necessarily just on soda-lime glasses (Wang et al. 2008; Sant et al. 2007; Scarso and Decamps 2007; Ewald et al. 2006; Sangpour et al. 2009).

These two techniques are completely different. The first one is based on radio frequency (RF) co-sputtering of silver and silica targets, while the second one is based on chemical solution of silver-based salts in the sol and subsequent reduction of Ag ions to the metallic state by a reducing agent (De et al. 1996; Mennig et al. 1997; Kawashita et al. 2000). Sputtered layers do not need post-deposition densification, thus making this technique suitable for every substrate (Balagna et al. 2012).

A comprehensive characterization of silver/silica antibacterial coatings sputtered on silica substrates have been recently reported in Ferraris et al. (2008, 2010a, b, 2011).

Soda-lime glasses have been chosen for this work since they are the most widely used glasses and several attempts of conferring soda-lime glasses an antibacterial activity recently received international attention (Borrelli et al. 2012, http://www.agc-flatglass.sg/products-detail.aspx?id=32).

Coatings obtained by sputtering silver/silica composites on soda-lime and on silica substrates will be described in this paper by comparing results of several characterization techniques such as UV–visible spectroscopy (UV–Vis), X-ray diffraction (XRD), X-ray photoelectron spectroscopy (XPS), and Time of Flight-Elastic Recoil Detection Analysis (TOF-ERDA). The measurements were performed on as-deposited sputtered coatings and after heating them in air in the range of 150–450 °C, in order to investigate their structure and antibacterial behaviour. Mechanical properties measured by tape adhesion nanoindentation and scratch resistance tests will be investigated in order to quantify the sputtered coatings mechanical stability. Results will be compared with literature on sol–gel deposited silver/silica coatings on soda-lime glasses (Durucan and Akkopru 2010).

Materials and methods

Silver nanocluster/silica composite coatings were deposited on soda-lime (Knittel Glaser, Germany)

and on silica (Infrasil^{TM} substrates (25 mm $\times$ 25 mm) by RF co-sputtering (Microcoat MS450). Silver (Sigma-Aldrich 99.99 % purity) and silica (Franco Corradi S.r.l. 99.9 % purity) targets were used as described in Ferraris et al. (2010b). Coating thickness between 50 and 300 nm have been obtained varying deposition time.

Their thickness has been measured by contact profilometry (KLA-Tencor P15) after deposition on partially masked samples, by measuring the step height between the coated and uncoated substrate.

About ten samples per temperature were heated up from 150 to 450 °C, 1 h dwelling time, in a muffle furnace in air and then characterized.

As-deposited and heated samples were characterized by UV–Vis absorption spectroscopy (Varian Cary 300 Bio Agilent Technologies Company), XRD (PW3040/60 X'Pert PRO MPD from PANalytical in Thin Film geometry, integration time 80 s, step 0.02°) and XPS analysis (VSW-XPS system equipped with a non-monochromatic Al K$_\alpha$ source and a Concentric Hemispherical Class 100 Analyzer). No particular sample preparation was required for these kinds of measurements.

Quantitative surface compositions were determined for all samples from high resolution scans of the O 1s, Si 2p, C 1s, Na 1s and Ag 3d spectral regions, using step size of 0.2 eV and a pass energy of 22 eV. The binding energy (BE) was referenced to the C 1s line at 285 eV and charge corrections were performed accordingly.

The chemical analyses carried out with the non-monochromatic source were integrated with detailed measurements of the photoelectron spectra of silver nanocluster/silica composite coatings as-deposited on silicon, using an ESCA200 Scienta apparatus equipped with a monochromatized Al K$_\alpha$ X-ray source and a charge compensator (Speranza et al. 2009).

TOF-ERDA measurements were performed using 20 MeV I ions from the 6 MV Tandem Van de Graaff accelerator at the Ruder Boskovic Institute in Zagreb (Siketic et al. 2010). The beam current during the measurement was kept around 3 nA. To detect atoms recoiled from the target, TOF-ERDA detector was placed at 37.5° and the angle between the beam and the sample surface during the measurements was 20°.

In order to evaluate the antimicrobial properties of the coatings, as-deposited and heat-treated samples (60 nm thick) have been subjected to the inhibition halo test, in accordance to the National Committee for

Clinical Laboratory Standards (NCCLS) (NCCLS M2-A9) A gram-positive bacterium, *Staphylococcus aureus* (*S. aureus*, ATCC 29213), and a fungus, *Candida albicans* (*C. albicans*), were used.

Moreover, the count of adhered colonies forming units (CFU) has been performed to evaluate the ability of as-deposited and heat-treated samples to limit the bacterial contamination (NCCLS M7-A6). In this case a *S. aureus* strain has been selected and a control sample (soda-lime glass without coating) has been used. Tests have been performed in triplicate, as described in Ferraris et al. (2010b). All products have been purchased from BD-Becton–Dickinson, USA.

Cross-cut tape tests have been performed according to ASTM 3359 (ASTM D 3359-97) in order to investigate the coating adhesion to the soda-lime substrate. A grid of parallel cuts has been done on the coated surface by a cutter. Surface has been cleaned with a brush and the tape applied on the grid. After tape removal coating damage into the grid has been visually determined with a lens and compared to the reference reported in the standard (ASTM D 3359-97).

Ageing tests have been performed according to ASTM 1087 standard (ASTM C 1087). As-deposited and thermally treated samples (150–450 °C) have been fixed to metallic supports and introduced into a climatic chamber (QUV Weathering Tester) and subjected to UV-A irradiation and humidity cycles (100 % humidity, 4 h) up to 500 h. The mean energy of UV irradiation was 0.75 W/m^2/nm at the test temperature of 50 °C.

Coating resistance to several common sterilization processes such as steam, radiation and chemical sterilization has been tested: steam sterilization in autoclave (Asal 760) through a 15-min cycle at 121 °C and 1 atm of pressure; 25 kGy gamma ray irradiation (Gammatom s.r.l., Guanzate—CO, Italy); ethylene oxide (EtO standard cycle, Bioster S.p.a., Seriate—BG, Italy). Samples have been packed in sterilization bags for these tests. Samples have been visually inspected in order to determinate significant alteration and/or detachment of the coating; tape tests have been done on samples before and after sterilization to verify the coating adhesion.

Scratch tests have been performed in Revetest mode (Revetest, CSM Instruments). A progressively increasing load (from 0 to 50 N) has been applied to coated surface by means of a Rockwell C diamond indenter with a 200 μm diameter, through a 5-mm

track. No particular sample preparation was required for this measurement. Three different tracks have been performed on each sample. The whole morphology of the track has been recorded, during optical microscope observation and critical loads were determined through acoustic emission (AE) measurements and optical observations of the scratch. Coating resistance has been evaluated comparing the critical loads of the different samples (Le Houerou et al. 2003).

Morphology and chemical composition in and out of the scratch tracks have been evaluated by scanning electron microscopy equipped with energy dispersive X-ray spectroscopy (SEM-FEI, QUANTA INSPECT 200, and EDS-EDAX PV 9900). Samples have been sputter-coated with a thin Cr layer in order to make them conductive for SEM observations.

Nanoindentation tests have been done on as-deposited and heated (450 °C) coatings deposited on silica and soda-lime substrates by a nanoindenter (NanoTest^{TM} platform) with a Berkovic tip. No particular sample preparation was required for this test.

Two different kinds of test were performed for each sample. Depth-controlled mode, where the maximum indentation depth is fixed (in these measurements 30 and 50 nm were set as indentation depth); and load-controlled mode, where the maximum applied load during indentation was fixed (in these measurement 1 and 5 mN were set as applied load). The other parameters were: indenter contact velocity (0.1 μm/s), load time (20 s), unloading time (15 s) and dwell time at maximum load (10 s).

Results

Sputtered coatings morphology

The visual appearance of the as-sputtered and heated silver nanocluster/silica composite coated soda-lime is shown in Fig. 1: a darker colour is evident in the as-deposited sample, which slightly decreases intensity after heating from 150 to 450° C. This is due to different clusters dimension (increase with thermal treatments) that leads to different Localized Surface Plasmon Resonance (LSPR) effect.

The sputtered coatings consist in a silica matrix embedding silver nanoclusters with dimension ranging from 1 to 50 nm, according to the heat treatment, as visualized by high resolution transmission electron microscopy (HR-TEM) on silica substrates (Ferraris et al. 2010a). Field emission scanning electron microscopy (FESEM) (Fig. 2) on soda-lime substrates was made on the cleaved section of as-deposited coatings (Fig. 2a), which shows some bright areas in a silica matrix. After heating at 450 °C (Fig. 2b), a few silver nanoclusters on the surface and a bright line are evident.
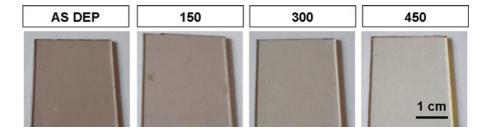
UV–Vis

The UV–Vis spectra of the as-sputtered and heated silver nanocluster/silica composite on soda-lime substrates are reported in Fig. 3a (on silica substrates in Fig. 3b for comparison purposes).

The curves are normalized to the maximum peak which corresponds to the as-deposited one for the coatings on soda-lime (Fig. 3a) and to the heated at 450 °C for those on SiO$_2$ (Fig. 3b), respectively.

In both the depositions, the local minimum at around 320 nm corresponds to the wavelength at which the real and imaginary parts of the silver dielectric function vanish; the absorption at shorter wavelengths is mainly due to the intra-band electronic transitions of silver (Sosa et al. 2003).

The absorption curves of coatings on soda-lime (Fig. 3a) show absorption peaks shifting from 403 to 423 nm, which gradually lower their intensity from the as-deposited coating to the heat-treated ones. The peak becomes much sharper for the 450 °C heated sample, which has also the lightest colour (see Fig. 1).

Fig. 1 Silver nanocluster/silica composite coatings on soda-lime glasses as-deposited and after thermal treatments
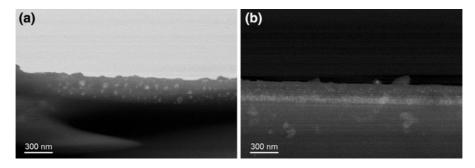
Fig. 2 FESEM on silver nanocluster/silica composite coating cross section on soda-lime glasses as-deposited (**a**) and after thermal treatment at 450 °C (**b**)

On the contrary, the spectra of Fig. 3b, referring to the same silver nanocluster/silica composites sputtered on silica substrates, show a gradual increase of the absorption peaks from the as-deposited coating to the heated ones, with an evident peak absorption increase after heating at 450 °C, as reported also in Ferraris et al. (2010a).
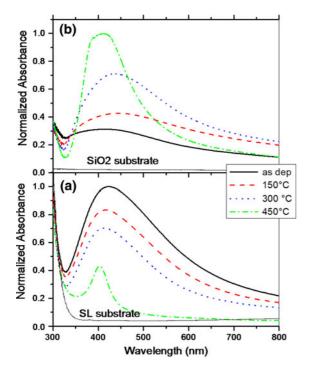

Fig. 3 UV–Vis absorption spectra of silver nanocluster/silica composite coatings on soda-lime (**a**) and silica (**b**) substrates, evidencing the silver nanoclusters Localized- Surface Plasmon Resonance absorption peaks, as-deposited and after thermal treatments. The *curves* are normalized to the maximum of the as-deposited sample for the coatings on soda-lime and to the maximum of the sample heated at 450 °C on SiO$_2$

XRD

XRD broad peaks due to silica amorphous matrix, and peaks related to metallic silver, ($2\theta = 38.15°$, JCPDS card no. 4-0783), corresponding to Ag (111) are present in both as-deposited coatings sputtered on soda-lime and on silica substrates (Fig. 4a, b, respectively). Metallic silver peaks gradually increase and then decrease their intensity from the as-deposited to the heat-treated at 450 °C, only when deposited on the soda-lime substrate (Fig. 4 a).

When the soda-lime substrate is replaced by a silica one (Fig. 4b), the silver XRD absorption has the already reported trend (Ferraris et al. 2010a, b); metallic silver peaks gradually increase their intensity from the as-deposited coating to the heat-treated ones up to 450 °C.

XPS and TOF-ERDA

XPS analyses showed the presence of Ag, Si, Na, O and adventitious C on the surface of as-deposited and heated sputtered silver nanocluster/silica composite coatings on soda-lime (Fig. 5a) and on silica (Fig. 5b). Curves have been vertically shifted for an easier reading.

Table 1 gives a summary of the atomic surface composition as calculated by XPS for silver nanocluster/silica composite coatings on soda-lime and on silica substrates, as-deposited and after thermal treatments.

For sputtered coatings on soda-lime substrates it is striking to observe the surface increase of Na/Si ratio and the corresponding decrease of Ag while heating at 300 and 450 °C, respectively. On the contrary, the Ag/Si ratio is constant within the experimental variation
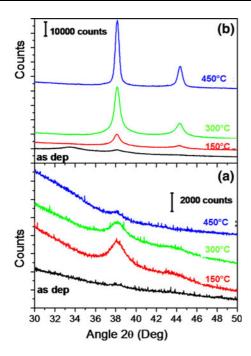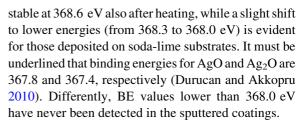
Fig. 4 XRD patterns of silver nanocluster/silica composite coatings on soda-lime (**a**) and on silica (**b**) substrates, as-deposited and after thermal treatments

for silica substrates. In both cases, the O/Si ratio is close to that of silica, again, within the experimental uncertainty.

This feature is observable with more detail in Fig. 6a, b for silver nanocluster/silica composite coatings on soda-lime glasses: the intensity of the Ag $3d_{5/2}$ core line decreases from as-deposited samples to those heated at 450 °C (Fig. 6a), after an initial slight increase for samples heated at 150 and 300 °C. On the same samples, the Na 1s peak appears at 150 °C and gradually increases intensity up to 450 °C (Fig. 6b). The curves have been normalized to the intensity of the Si_{2p} peak.

BEs for Ag $3d_{5/2}$ core lines of the sputtered coatings on soda-lime glasses and on silica are shown in Table 1: due to the dielectric nature of the samples, charge effect corrections made impossible to obtain an accuracy better than 0.2 eV. However, the BE for silver on the surface of both coatings are slightly higher than the literature value of metallic silver (Ag[0], 368.2 eV), (Durucan and Akkopru 2010), with an average of 368.3 eV for coatings on soda-lime and 368.6 eV on silica, respectively.

Moreover, the BE of Ag $3d_{5/2}$ on the surface of coatings deposited on silica substrates is remarkably

stable at 368.6 eV also after heating, while a slight shift to lower energies (from 368.3 to 368.0 eV) is evident for those deposited on soda-lime substrates. It must be underlined that binding energies for AgO and Ag_2O are 367.8 and 367.4, respectively (Durucan and Akkopru 2010). Differently, BE values lower than 368.0 eV have never been detected in the sputtered coatings.

TOF-ERDA, on as-deposited sputtered coatings and after heating in air in the range of 150–450 °C (Fig. 12a, b) shows the concentration profiles of Na and Ag. A decrease of silver and corresponding increase of sodium is evident on heated samples.

Antibacterial tests

Figure 7 shows the results of the inhibition halo test performed on sputtered silver nanocluster/silica composite coatings on soda-lime glasses, as-deposited and on heat-treated samples, both for *S. aureus* and *C. albicans* strain. It can be observed that the as-deposited and annealed samples up to 300 °C are able to create an inhibition halo of about 1 mm. Samples annealed at 450 °C are not able to create an inhibition zone around the sample, nevertheless bacteria do not proliferate under it.

A significant reduction of adhered Colonies Forming Units (CFU) has been observed on the coated samples respect to the control sample. The percentage of reduction is about 90 % for as-deposited samples and for samples heated up to 300 °C, while it is only 50 % for samples heat treated at 450 °C.

The percentage reduction has been calculated as:

$$(CFU_c - CFU_x / CFU_c) \times 100$$

where CFU_c is the number of colonies forming units counted on the control sample and CFU_x is the number of bacterial colonies counted on coated samples.
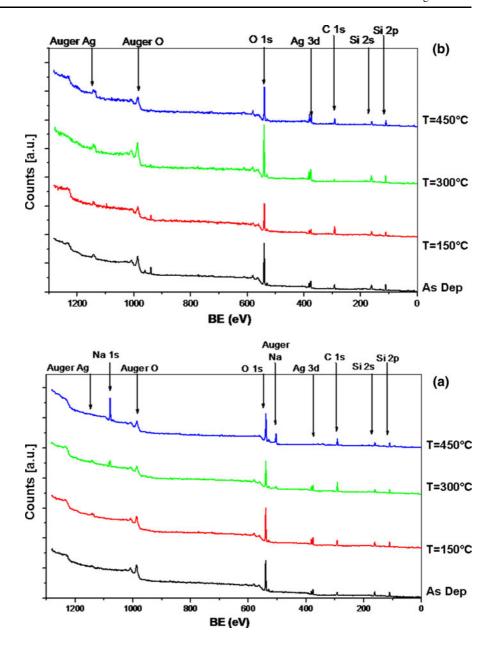
Tape tests before and after ageing and sterilization

Figure 8 (first row) reports the visual inspection of sputtered silver nanocluster/silica composite coatings on soda-lime glasses (as-deposited and thermally treated) after tape test, together with tapes after removal. It can be observed that no damage has been induced on all samples and all tapes are clean from coating detached parts.

Figure 8 (from second to fifth rows) shows a qualitative comparison of samples before and after

Fig. 5 XPS survey spectra of silver nanocluster/silica composite coatings on soda-lime glasses (**a**), and on silica (**b**) as-deposited and after thermal treatments (*curves* have been shifted for an easier reading)

Table 1 Main stoichiometric ratios and Ag 3d$_{5/2}$ binding energy of silver nanocluster/silica composite coatings on soda-lime glasses and silica as deposited and after thermal treatments

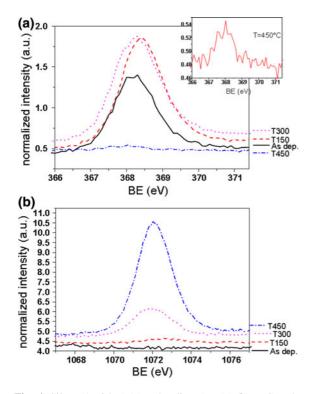|	Soda-lime				SiO$_2$		
	Ag/Si	Na/Si	O/Si	B.E. Ag 3d$_{5/2}$ (eV)	Ag/Si	O/Si	B.E Ag 3d$_{5/2}$ (eV)
As-dep	0.06 ± 0.02	–	2.04 ± 0.04	368.3	0.09 ± 0.02	2.21 ± 0.05	368.6
$T = 150$ °C	0.10 ± 0.02	–	2.18 ± 0.05	368.4	0.08 ± 0.03	2.19 ± 0.06	368.7
$T = 300$ °C	0.10 ± 0.03	0.28 ± 0.03	2.25 ± 0.07	368.3	0.11 ± 0.02	2.20 ± 0.04	368.6
$T = 450$ °C	<0.02	0.82 ± 0.04	2.36 ± 0.07	368.0	0.15 ± 0.02	2.16 ± 0.05	368.6

Fig. 6 Silver (Ag 3d$_{5/2}$) (**a**) and sodium (Na 1s) (**b**) XPS peaks in silver nanocluster/silica composite coatings on soda-lime glasses as-deposited and after thermal treatments. The *inset* shows the spectra after the annealing at 450 °C. The *curves* have been normalized to the intensity of the Si 2p peak

some common ageing and sterilization processes. It can be observed (second and third rows) that coatings are discoloured by the UV-humidity ageing and autoclave sterilisation with significant damage of the coating, which is partially removed; their antibacterial

activity (not reported here) vanished. Considering the significant macroscopic damage, no tape tests have been done on these samples.

After gamma irradiation (Fig. 8, fourth row) and ethylene oxide sterilizations (Fig. 8, fifth row), no detectable variation in the coating visual appearance has been revealed for both as-deposited and thermally treated samples. A moderate darkening of samples can be noticed after gamma irradiation and can be attributed to the colour change of gamma irradiated glasses, widely documented in literature (Narayan et al. 2008, Ezz-Eldin et al. 2008).

Tape tests after gamma (Fig. 8, fourth row) and EtO (Fig. 8, fifth row) sterilizations indicate that adhesion of the coating remains unchanged after these processes.
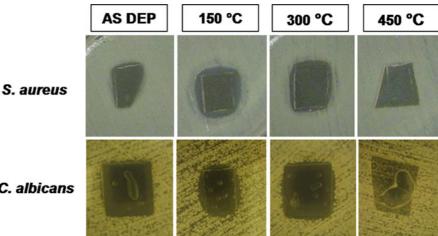
Scratch tests

Figure 9 shows results of the scratch test tracks of as-deposited and thermally treated samples. The appearance of the first circular crack (Hertzian crack) has been considered as a parameter for the evaluation of coating mechanical properties versus thermal treatment.

The as-deposited sample showed the appearance of the first circular crack at the highest load (Fig. 9a), which slowly decreases up to a minimum for the coating heated at 450 °C.

SEM observations and EDS analyses of the scratch tracks (Fig. 10) indicate that the coating is just cracked and not removed at the appearance of the first crack and that silver is still detectable inside the track.

Fig. 7 Silver nanocluster/ silica composite coatings on soda-lime glasses as-deposited and after thermal treatments: inhibition halo for *S. aureus* and *C. albicans*
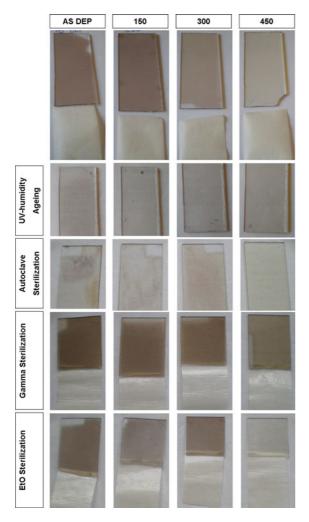
Fig. 8 Silver nanocluster/silica composite coatings on soda-lime glasses as-deposited and after thermal treatments: effects of ageing and different sterilization processes on tape test results

Nanoindentation tests

Nanoindentation tests have been done on as-deposited and heated coatings (450 °C) on silica and soda-lime substrates: Fig. 11 shows the hardness of the uncoated substrates (for comparison purposes) and of the as-deposited and heated coatings, together with the depths and loads reached during the test.

The same trend and considerations observed for the hardness have been measured also for the reduced modulus (not reported here) which is related to the material Young modulus, also taking into account the indenter material characteristics (Almasri and Voyiadjis 2010; Lucca et al. 2010).

Discussion

Sputtered coatings morphology

The use of a silica target instead of a silicon one, allows to obtain coatings made of silver nanoclusters embedded in a silica matrix by a one-step sputtering process without need of oxidation/reduction treatments, as in Sangpour et al. (2009).

The characteristic darker (brownish) colour due to the presence of silver nanoclusters is evident in Fig. 1 for sputtered silver nanocluster/silica composite coatings on soda-lime, as already discussed for the same coatings, but sputtered on silica substrates. The slight decrease of colour intensity after heating in air is due to size modification of the nanoclusters (Ferraris et al. 2010a, b).

Differently from what reported in Durucan and Akkopru (2010) for sol–gel coatings, sputtered coatings are crack-free (Fig. 2a), and silver nanoclusters are clearly visible by FESEM after heating them 1 h in air up to 450 °C (Fig. 2b).

Heat treatments have been performed in order to test the antibacterial activity after heating, not to improve the coating cohesion or adhesion to the substrate, as will be discussed in the following paragraphs.

The morphology shown in Fig. 2a is not directly related to silver nanoclusters, probably because of the cleavage; however, a silica matrix embedding silver nanoclusters is clearly observed on samples heated at 450 °C (Fig. 2b). This morphology corresponds to what reported in Ferraris et al. (2010a, b).

A very interesting bright line is evidenced in Fig. 2b for the sputtered coatings heated at 450 °C, a proof of the ionic exchange occurred between the sputtered coating and the soda-lime substrate. Silver ions diffuse from the coating toward the soda-lime substrate by ion-exchange reaction with sodium ions, which diffuse from the soda-lime substrate to the coating: a higher concentration of silver ions away from the coating surface and deeper toward the soda-lime substrate is evidenced by the bright line.

The ionic-exchange process occurring here by simple heating may be of interest for optical applications, as also reported in Jimenez et al. (2011); moreover, it can be used to obtain buried optical waveguides, thus avoiding the double ionic exchange process usually requested to obtain them.
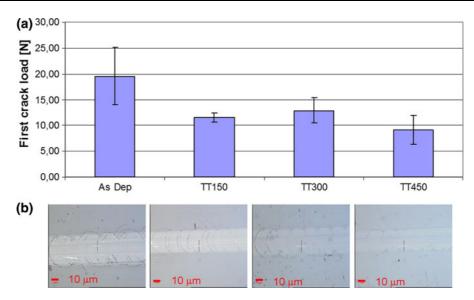
Fig. 9 Scratch tests on silver nanocluster/silica composite coatings on soda-lime glasses before and after thermal treatment: **a** comparison of first crack load and **b** morphology of the first crack

UV–Vis

The UV–Vis absorption spectra of silver nanocluster/ silica composite coatings on soda-lime substrates after different thermal treatments (Fig. 3a) show absorption peaks ranging from 423 to 403 nm (Fig. 3b on silica substrates for comparison purposes). These signals are due to the well-known LSPR absorption of metal silver nanoclusters of composite coatings (Hoa et al. 2007).

The LSPR absorption is higher for the as-deposited coating on soda-lime and gradually lower for the heat-treated ones, up to a minimum absorbance and bandwidth for the 450 °C heated sample (Fig. 3a), which also shows a partial bleaching in Fig. 1.

On the contrary, Fig. 3b (coatings deposited on silica) shows the expected gradual increase of the silver nanocluster LSPR absorption from the as-deposited coating to the heated ones, with an evident peak increase after heating at 450 °C, as already discussed in Ferraris et al. (2010a).

The difference in LSRP absorption between coatings sputtered on soda-lime (Fig. 3a) and those on silica substrates (Fig. 3b) after heating at temperature higher than 300 °C can be due to the ionic exchange process Na^+/Ag^+. The process occurs between the soda-lime substrate and the sputtered silver nanocluster/silica composite coatings, as evidenced by FESEM (Fig. 2b).

This process is also reported in Durucan and Akkopru (2010) and Jimenez et al. (2011) for sol–gel silver/silica coatings deposited on soda-lime substrates. Differently from what reported in Durucan and Akkopru (2010), Ag^+ ions have never been detected by UV–Vis on silver nanocluster/silica composite coatings sputtered on silica (Ferraris et al. 2010a). Here, the Ag^+ absorption at 305 nm (Ferraris et al. 2010a, b, 2011) cannot be detected by UV–Vis spectroscopy, due to the soda-lime cutoff at 340 nm (Fig. 3a).

An ionic exchange process in the range of 300–450 °C is consistent with the typical Na^+/Ag^+ ionic exchange temperatures for soda-lime glasses with molten salts (Borrelli et al. 2012). For these coatings, the Na^+/Ag^+ ionic exchange should involve the Ag^0/Ag^+ equilibrium (Jimenez et al. 2011), as discussed also in Bi et al. (2002). Oxidation is possible in air above 200 °C for Ag particles smaller than a critical value, compatible with the size of silver nanoclusters present in the sputtered coatings. Hence, a gradual shift of the Ag^0/Ag^+ equilibrium toward Ag^+, thus decreasing the Ag^0 LSPR peak absorption can occur. Ag^+ is quickly replaced by Na^+ ions by ionic exchange with the soda-lime substrate. Ag^+ ions diffuse away from the coating inside the soda-lime glass and Na^+ ions move from the soda-lime through the sputtered coating, as reported in Jimenez et al. (2011), where these coatings were studied for photonic applications.

Since the LSPR absorption after heating at 450 °C is of lower intensity and of smaller bandwidth

Fig. 10 Scratch tracks on silver nanocluster/silica composite coatings on soda-lime glasses as-deposited and after thermal treatments: SEM images (**a**) and EDS analyses in the track (**b**) and out of it (**c**)

(Fig. 3a), but still present, it means that just a part of silver undergoes to oxidation, the rest remains as metallic silver nanoparticles.

When the soda-lime substrate is replaced by a silica one, the ionic exchange discussed above is obviously impossible and the silver LSPR absorption (Fig. 3b)

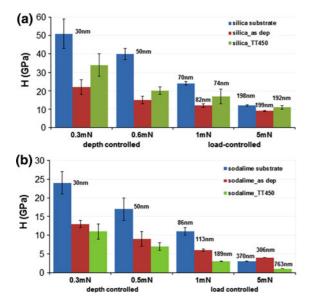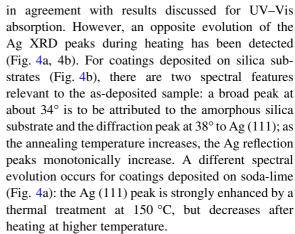**Fig. 11** Hardness of silver nanoclusters silica composite layers on silica (**a**) and soda-lime (**b**) substrates

has the well-known trend, in agreement with the nanocluster size increase during heat treatment. It means an increase of the LSPR absorption and decrease of its bandwidth (Ferraris et al. 2010a, b; Mattei et al. 2007).

A demonstration of Ag^+/Na^+ ionic exchange for sol–gel silver/silica coatings deposited on soda-lime substrates has been thoroughly discussed in Durucan and Akkopru (2010): it was observed during heating at temperatures higher than 500 °C necessary to densify these sol–gel coatings. However, a completely different trend in UV–Vis absorption spectra have been reported in Durucan and Akkopru (2010), due to the preparation of the sol–gel coatings which is completely different from sputtering and gave Ag^+ rich coatings; sol–gel coatings gave an oscillating and reversible silver SPR, clearly increasing the 412 nm SPR absorption only after heating at 700 °C. The complex reactions occurring during heating of silver/silica sol–gel coatings (Durucan and Akkopru 2010), involving atomic silver, ionic silver and silver nanoparticles can explain the different trend in the UV–Vis spectra of sol–gel and sputtered silver/silica coatings.

XRD

XRD peaks due to metallic silver have been detected in our coatings, as-deposited and after heating, both when sputtered on soda-lime and on silica substrates,

in agreement with results discussed for UV–Vis absorption. However, an opposite evolution of the Ag XRD peaks during heating has been detected (Fig. 4a, 4b). For coatings deposited on silica substrates (Fig. 4b), there are two spectral features relevant to the as-deposited sample: a broad peak at about 34° is to be attributed to the amorphous silica substrate and the diffraction peak at 38° to Ag (111); as the annealing temperature increases, the Ag reflection peaks monotonically increase. A different spectral evolution occurs for coatings deposited on soda-lime (Fig. 4a): the Ag (111) peak is strongly enhanced by a thermal treatment at 150 °C, but decreases after heating at higher temperature.

Differently for what reported in Durucan and Akkopru (2010), where only one broad peak representing amorphous silica is detectable for the as-deposited silver/silica sol–gel layers, metallic silver XRD peaks are already present in the as-sputtered coatings on soda-lime and silica substrates (Fig. 4a, b). This difference is due to the already mentioned differences between sputtering and sol–gel methods. With sputtering, two targets (metallic Ag and vitreous silica) are used to co-deposit silver nanocluster/silica composites: the expected composition of the resulting composite is a silica matrix embedding metallic silver nanoclusters, as in Ferraris et al. (2010a, b, 2011) and Balagna et al. (2012). Sol–gel is based on chemical reactions of products containing ionic silver, gradually reduced to the metallic form during complex drying and calcination processes. It is thus consistent to have metallic silver species less abundant in a sol–gel coating than in a sputtered one.

Another difference from Durucan and Akkopru (2010) is that the sol–gel coating calcination forms metallic silver peaks up to 700 °C. In our coatings sputtered on soda-lime, there is the slowly decrease of the metallic silver XRD peak from the as-deposited coatings to the heat-treated at 450 °C, as shown in Fig. 4a.

This behaviour is in accordance with the LSPR absorption evolution: during heating, an ionic exchange process Na^+/Ag^+ occurs between the sputtered coatings and the soda-lime substrate, gradually shifting the Ag^0/Ag^+ equilibrium toward Ag^+ thus decreasing the Ag XRD diffraction peak intensity; Ag^+ is quickly replaced by Na^+ ions by ionic exchange with the soda-lime substrate, as also discussed in Jimenez et al. (2011).

Since the sol–gel coatings on soda-lime substrates are cracked (Durucan and Akkopru 2010) their adhesion to the soda-lime substrates might be lower than for the sputtered coatings. The metallic silver XRD peak increases its intensity up to 700 °C for sol–gel coatings because the thermal reduction of the abundant ionic silver to metallic state is the main reaction here. The lower contribution of the Na^+/Ag^+ ionic exchange process may be due to the poor adhesion of the sol–gel coatings to the soda-lime substrate.

On the contrary, a gradual shift of the Ag^0/Ag^+ equilibrium toward Ag^+, together with the Na^+/Ag^+ ionic exchange, give the strongest contribution to reactions occurring between 300 and 450 °C for the sputtered coatings, because of their better adhesion on soda-lime substrates. The XRD (and LSPR) peaks decrease consequently.

When the soda-lime substrate is replaced by a silica one, the ionic exchange is obviously impossible and the silver XRD absorption of the sputtered coatings has the already discussed increasing trend (Ferraris et al. 2010a, b). Metallic silver XRD peaks gradually increase their intensity from the as-deposited coating to the heat-treated ones, due to the nanocluster size increase.

Finally, the presence of metallic silver already available in the as-sputtered coatings, without heat treatments needed, makes this technique suitable also to coat polymers (Balagna et al. 2012).

XPS and TOF-ERDA

XPS analyses and approximate surface composition showed a remarkable difference between coatings sputtered on soda-lime (Fig. 5a) and on silica substrates (Fig. 5b): there is an evident increase of Na 1s and corresponding decrease of Ag 3d doublet while heating from 300 to 450 °C for coatings sputtered on soda-lime. On the contrary, Fig. 5b (silica substrates) and Table 1 clearly show that, with silica substrate, the Ag/Si ratio remains approximately constant, clearly supporting the hypothetical ionic exchange discussed before and in Durucan and Akkopru (2010) to explain FESEM, UV–Vis and XRD results.

The approximate surface chemical composition of the sputtered coatings on soda-lime after heating at 450 °C has a remarkable similarity with results reported in Durucan and Akkopru (2010) for samples calcined at 500 °C. This evidence supports the existence of an ionic exchange process occurring on both sol–gel and sputtered coatings on soda-lime substrates.

This feature is observable with more detail in Fig. 6a, b, where the Ag $3d_{5/2}$ and Na 1s core peaks normalized to the relevant Si 2p peak, are reported at different thermal treatments: for coatings on soda-lime glasses (Fig. 6a), the silver peaks due to Ag $3d_{5/2}$ decreased intensity when samples are heated at 450 °C. The Na (1s) peak appears at 150 °C and gradually increases intensity up to 450 °C (Fig. 6b), thus confirming the supposed Ag^+/Na^+ ionic exchange up to the surface of these samples with consequent surface compositional change (i.e. lower silver concentration).

The gradual increase of Ag $3d_{5/2}$ peaks from as-sputtered to 300 °C samples, then a decrease when heated at 450 °C (Fig. 6a) is in agreement with oxidation versus ion exchange competing processes, also reported in Jimenez et al. (2011).

In order to further confirm the Ag^+/Na^+ ionic exchange, TOF-ERDA measurements have been done on sputtered coatings on soda-lime glasses, as-deposited and post-thermal treatments (Fig. 12). The experimental setup was optimized to analyse about 500 nm of the coating thickness.

Ag and Na profiles measured by TOF-ERDA show a migration of silver from the surface towards the bulk. A gradual decrease of Ag concentration can be seen if we compare as-sputtered and heated samples. The lowest Ag concentration was measured for samples heated at 450 °C. In this case, the silver concentration is lower at the surface and reaches a maximum deeper in the sample (Fig. 12a), as also evidenced by FESEM (Fig. 2b). This is consistent with the Ag^+/Na^+ ionic exchange, demonstrated here by the gradual increase of Na^+ on the same samples (Fig. 12b).

The average atomic percentage of the main elements (Ag, O, Na, Si) as determined by TOF-ERDA analyses (listed in Table 2) confirms the opposite trend of Ag and Na content as function of the heating temperature. TOF-ERDA results are in agreement with what discussed above about FESEM, UV–Vis, XRD and XPS on these layers.

The differences in ratios calculated by XPS (Table 1) and TOF-ERDA (Table 2) on the same samples are due to the fact that XPS analyses a few nanometers on the surface, while TOF-ERDA was optimized to analyse about 500 nm, thus the whole coating.
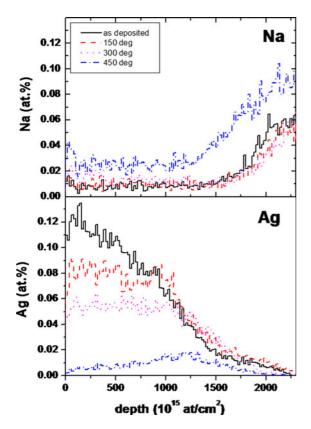
Fig. 12 TOF-ERDA concentration profile of Na (*top*) and Ag (*bottom*) for silver nanocluster/silica composite coatings on soda-lime glasses as-deposited and after thermal treatments

As already stated, the binding energies of the Ag $3d_{5/2}$ core lines are located in average at 368.3 eV for coatings on soda-lime and 368.6 eV on silica, respectively (Table 1) and they are slightly higher than the value of metallic silver ($Ag^0 = 368.2$ eV) and undoubtedly higher than the binding energies relevant to AgO (367.8 eV) and Ag_2O (367.4 eV) (Durucan and Akkopru 2010, http://srdata.nist.gov/xps/selEnergyType.aspx).

It is also clear from Durucan and Akkopru (2010) that sol–gel layers generally have lower BE, both as-

deposited and after the same thermal treatment, in agreement with those discussed above about the intrinsic difference of the two methods.

In order to understand why BE for Ag $3d_{5/2}$ are slightly higher than the literature value of metallic silver, silver nanocluster/silica composite coatings have been sputtered on pure monocrystalline silicon (to avoid any possible reaction between sputtered coating and substrate) and measured by a Scienta Gammadata ESCA 200 Uppsala Sweden, equipped with a monochromatic Al Kα X-ray source. The spectral resolution was about 0.3 eV (measured at the Ag Fermi edge) and the accuracy was better than 0.1 eV. Figure 13 shows the perfectly symmetric peak at 368.5 eV for Ag $3d_{5/2}$, with no components lower than 368.0 eV, thus confirming the previous results and the composition of the as-deposited layers composed by silica and metallic silver.

Moreover, a quantum confinement effect, typical of metal nanoclusters smaller than 5 nm, has been observed by the XPS valence band spectra and shown in Fig. 14. The spectrum of the as-sputtered coating shows a loss of feature with respect to that of pure silver (Ag Ref, deposited by thermal evaporation). Its valence band width is around 1.6 eV, in excellent agreement with Speranza et al. (2009), Minati et al. (2008, 2010) and Wertheim et al. (1983) on silver nanoparticles embedded in a soda-lime glass.

This value is also in agreement with the morphology of the as-deposited coatings observed in cross section by transmission electron microscopy (Ferraris et al. 2010a).

To summarize results obtained by XPS and TOF-ERDA:

– Ag^+/Na^+ ionic exchange was evidenced by observing a gradual decrease of Ag 3d doublet and a corresponding increase of Na, only on coatings sputtered on soda-lime, after heating up to

Table 2 Compositional analysis as calculated from TOF-ERDA profiles (at.%) of silver nanocluster/silica composite coatings on soda-lime glasses as-deposited and after thermal treatments

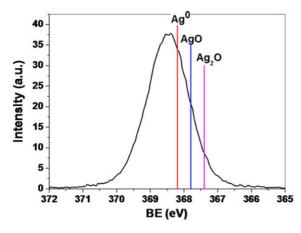|	O (%)	Na (%)	Si (%)	Ag (%)	Ag/Si	O/Si	Na/Si
As-dep	56.6 ± 2.0	0.8 ± 0.2	27.4 ± 1.4	10.9 ± 1.0	0.40 ± 0.04	2.07 ± 0.13	0.03 ± 0.01
150 °C	58.9 ± 1.9	1.0 ± 0.3	25.9 ± 1.5	7.8 ± 0.8	0.30 ± 0.04	2.27 ± 0.15	0.04 ± 0.01
300 °C	59.2 ± 1.9	1.5 ± 0.4	26.7 ± 1.4	5.5 ± 0.4	0.21 ± 0.02	2.22 ± 0.14	0.06 ± 0.02
450 °C	61.3 ± 2.1	2.5 ± 0.5	26.9 ± 1.2	0.6 ± 0.1	0.022 ± 0.004	2.28 ± 0.13	0.09 ± 0.02
SL	60.3 ± 2.0	8.4 ± 1.6	26.9 ± 0.9	–	–	2.24 ± 0.11	0.31 ± 0.06

Fig. 13 Silver (Ag $3d_{5/2}$) XP spectrum relevant to as-deposited silver nanocluster/silica composite coating on silicon. The measurement was performed using a Scienta ESCA 200 analyzer (Gammadata, Sweden) equipped with a monochromatized Al K_α X-ray source, using a pass energy of 150 eV and a step size of 0.05 eV. The *vertical lines* show the positions of metallic Ag^0, AgO and Ag_2O peaks as derived from literature (http://srdata.nist.gov/xps/selEnergyType.aspx)
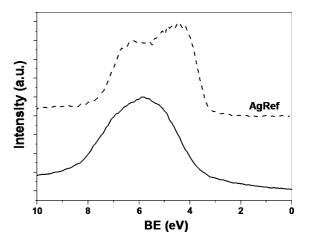

Fig. 14 XPS valence band of the silver nanocluster/silica thin film as-deposited on a silicon substrate measured using a Scienta ESCA 200 analyzer (Gammadata, Sweden) equipped with a monochromatized Al K_α X-ray source (pass energy 300 eV, step size 0.1 eV). The *upper* spectrum, shown for comparison purposes, is a reference silver metallic thin film (AgRef)

450 °C. These results have been confirmed by TOF-ERDA analyses.

– Ag $3d_{5/2}$ BE for coatings sputtered on soda-lime substrates have a 368.3 eV average value, with a minimum of 368.0 eV when these samples are heated at 450 °C

– a lower BE reveals a mixed chemical state for silver which is present both in metallic and oxide form on the surface

– the lower BE suggests that the metallic silver concentration on the surface must be lower at 450 °C, if compared to the as-sputtered one.

– an average 368.6 eV energy for Ag $3d_{5/2}$ on the surface of coatings sputtered on silica substrates reveals that silver is present in the metallic form

– this value is higher than the literature one for Ag $3d_{5/2}$ of metallic silver, due to the mean size (<5 nm) of silver nanoclusters obtained by sputtering

– this was confirmed by XPS analysis on coatings sputtered on silicon, where energy shifts and valence band due to quantum confinement effects have been observed

– this is consistent with the morphology reported in Ferraris et al. (2010a).

A similar XPS behaviour was reported by Durucan and Akkopru (2010), showing a Ag^+/Na^+ ionic exchange occurring between 300 and 700 °C on sol–

gel coated soda-lime samples and consequent surface composition change. Moreover, it was observed a BE shift to lower energy for the Ag 3d doublet, down to values of 374.10 eV (Ag $3d_{3/2}$) and 367.98 eV (Ag $3d_{5/2}$) for samples calcinated at 500 °C. This behaviour suggests the presence of abundant silver ions on the surface of sol–gel samples, if compared with the surface of the sputtered ones. The minimum BE was 368.0 eV for Ag $3d_{5/2}$, obtained when the coatings were sputtered on soda-lime substrates then heated at 450 °C.

All this is in agreement with the intrinsic differences of the sol–gel and sputtering deposition processes discussed before. However, a remarkable similarity has been evidenced in the ionic exchange process when both coatings are deposited on a soda-lime substrate, as also discussed by Jimenez et al. (2011) for photonic applications of these layers.

Finally, XPS confirmed ionic exchange and changes in the chemical state of silver during thermal treatments with different extent for both sputtered and sol–gel silver/silica coatings. A further confirmation will be given in the following paragraph on antibacterial activity of these layers.

Antibacterial tests

Since the interaction of Ag^+ ions with bacteria is restricted to the coating surface, the previous XPS and

TOF-ERDA characterization is fundamental to understand the results of the following antibacterial tests.

Results in Fig. 7 confirm that a heat treatment higher than 300 °C induces an ionic exchange process between the sputtered coatings and the soda-lime substrate, thus reducing the availability of silver on samples surface and consequently the antibacterial properties, as discussed above and in Durucan and Akkopru (2010).

Also the count of CFU test demonstrates these antibacterial properties of as-deposited and heat-treated samples up to 300 °C. A significant reduction (about 90 %) of adhered CFU has been observed between the control sample (uncoated soda-lime) and the sputtered samples (as-deposited and annealed up to 300 °C). The sample heated at 450 °C still reduces the CFU adhesion, but only of about 50 %. This is in full agreement with the previously discussed Ag^+/Na^+ ionic exchange, the consequent surface composition change evidenced by XPS and TOF-ERDA, and the residual presence of metallic silver in all samples, as detected by UV–Vis, XPS and XRD.

Again, a difference in antibacterial activity is evident between coatings deposited on soda-lime substrates and those deposited on silica substrates: after heating at temperature higher than 300 °C the antibacterial activity of coatings deposited on soda-lime substrates is reduced, while it is still evident on silica substrates after heating at 450 °C (Ferraris et al. 2010a).

This behaviour is also in agreement with results of Durucan and Akkopru (2010), where the antibacterial activity disappeared after calcination above 500 °C of the sol–gel layer deposited on soda-lime substrates.

It must be noted that the presence of silver inside the coating, but away from the surface, can be of low effect on its antibacterial activity, since the mobility of Ag^+ at room temperature is negligible. However, differently from Ag^+ inside an ion-exchanged glass (http://www.agc-flatglass.sg/products-detail.aspx?id=32) sputtered silver/silica coatings are characterized by a nanoporous silica matrix embedding Ag nanoclusters; consistently, these coatings have a non-negligible silver ion release even after heating at 450 °C (Ferraris et al. 2010a, b).

Tape tests before and after ageing and sterilization

Contrarily to what reported in Durucan and Akkopru (2010), the morphology of the sputtered silver nanocluster/silica composite coatings shows a good cohesion of the film and adhesion to silica (Ferraris et al. 2010a, b), polymer-substrates (Balagna et al. 2012) and soda-lime substrates (Ferraris et al. 2011). Because of this reason, some mechanical and durability tests have been done in view of a possible application of the sputtered antibacterial coatings to soda-lime surfaces.
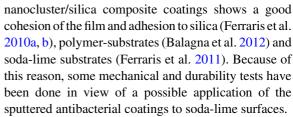
Figure 8 (first row) shows the sputtered coatings on soda-lime (as-deposited and thermally treated) after tape test: as-deposited and thermally treated (at all temperatures) can be classified as 5B (0 % damage) according to ASTM 3359, thus confirming the comment done in Ferraris et al. (2010b) about the good cohesion and adhesion of these sputtered layers on silica substrates.

Figure 8 (second and third rows) shows that the sputtered coatings can be damaged by the humidity plus UV ageing and autoclave sterilisation; significant damages have been observed, with the coating partially removed and the surface resulting irregular and spotted: the damage can be ascribed to humidity reactions with silica (Yang and Wang 2006), since same tests done with UV irradiation in dry conditions did not evidence any damage (unpublished results).

After both gamma irradiation and ethylene oxide sterilizations no visually detectable variation in the coatings appearance has been noticed for as-deposited and thermally treated samples.

Only after gamma irradiation a moderate darkening of samples can be seen (Fig. 8, fourth row): it can be ascribed to the formation of colour centres in the glass network of soda-lime substrate as widely reported in literature for gamma irradiation of glasses (Narayan et al. 2008; Ezz-Eldin et al. 2008).

Tape tests after gamma and EtO (Fig. 8 fourth and fifth rows) indicate that adhesion remains unchanged after these sterilization processes.

Scratch tests

Figure 9 shows results of the scratch test tracks of as-deposited and thermally treated samples.

The as-deposited sample showed the appearance of the first circular crack at the highest load (Fig. 9a), which slowly decreases up to a minimum for the coating heated at 450 °C; these results are confirmed by AE (not reported here).

The opposite behaviour (increasing of the first circular crack load vs heating) was measured and

discussed for the same coatings deposited on silica substrates in Ferraris et al. (2010b) as a result of densification.

A possible explanation can be the lower mechanical strength of the coating after the ionic exchange, which means an increased amount of Na^+, modifier of the silica network.

SEM observations and EDS analyses of the scratch tracks (Fig. 10) indicate that the coating is just cracked and not removed at the appearance of the first crack. Silver is still detectable inside the track, thus confirming the good cohesion of the sputtered coatings and their adhesion on soda-lime substrates.

Nanoindentation tests

Nanoindentation tests have been done on as-deposited and heated coatings (450 °C) deposited on silica and soda-lime substrates: Fig. 11 shows the measured hardness.

It is evident that heating at 450 °C has an opposite effect on the coating hardness: when deposited on silica, the coating hardness is improved by heating at 450 °C. The same heating at 450 °C on coatings deposited on soda-lime substrates gave opposite effects, in agreement with the above discussed Na/Ag ionic exchange, which weakens the silica amorphous network with the presence of Na^+ as a modifier. These results are in agreement with those discussed above for scratch tests.

Conclusions

Silver nanocluster/silica composite coatings were deposited in a less than two hours process on both soda-lime and silica glasses by RF co-sputtering, without densification post-treatment. The effect of thermal treatments on their microstructure in the range of 150–450 °C, the presence of silver ions and/or silver nanoclusters, the nanocluster size and their position inside the sputtered layers have been investigated by several characterization techniques (UV–Vis, XPS, XRD, TOF-ERDA) which evidenced a sodium/silver ionic exchange between the sputtered coatings and the soda-lime substrates after heating up to 450 °C.

The antibacterial activity of all coatings was verified against *S. aureus* and *C. albicans* by disk diffusion method and colonies forming units (CFU): in agreement with the microstructural results, the antibacterial activity present on all coatings was slightly reduced after heating at 450 °C. All coatings retained their antibacterial activity after gamma ray and ethylene oxide gas (EtO) sterilization. However, they resulted damaged by humidity plus UV ageing and by autoclave sterilization.

Tape resistance (ASTM D3359-97) nanoindentation and scratch resistance tests have been done on each coating, revealing a good adhesion on soda-lime substrates and a reduced hardness of the coating deposited on soda-lime substrates after heating at 450 °C.

References

Almasri AH, Voyiadjis GZ (2010) Nanoindentation in FCC metals: experimental study. Acta Mech 209:1–9

ASTM C 1087 Standard Test Method for determining compatibility of liquid-applied sealants with accessories used in structural glazing systems

ASTM D 3359-97 Standard test methods for measuring adhesion by tape test

Balagna C, Perero S, Ferraris S, Miola M, Fucale G, Manfredotti C, Battiato A, Santella D, Vernè E, Vittone E, Ferraris M, (2012) Antibacterial coating on polymer for space application. Mater Chem Phys 135:714–722

Bi HJ, Cai WP, Zhang LD, Martin D, Trager F (2002) Annealing-induced reversible change in optical absorption of Ag nanoparticles. Appl Phys Lett 81:5222–5224

Borrelli NF, Lathrop D, Senaratne W, Verrier F, Wei Y, (2012) Coated, antimicrobial, chemically strengthened glass and method of making. US Patent 2012/0034435

Brook LA, Evans P, Foster HA, Pemblec ME, Sheela DW, Steeleb A, Yates HM (2007) Novel multifunctional films. Surf Coat Technol 201:9373–9377

Castellano JJ, Shafii SM, Ko F, Donate G, Wright TE, Mannari RJ, Payne WG, Smith DJ, Robson MC (2007) Comparative evaluation of silver-containing antimicrobial dressings and drugs. Int Wound J 4:114–122

Chen W, Liu Y, Courtney HS, Bettenga M, Agrawal CM, Bumgardner JD, Ong JL (2006) In vitro anti-bacterial and biological properties of magnetron co-sputtered silver-containing hydroxyapatite coating. Biomaterials 27:5512–5517

De G, Tapfer L, Catalano M, Battaglin G, Gonella F, Mazzoldi P, Haglund RF Jr (1996) Formation of copper and silver nanometer dimension clusters in silica by the sol–gel process. Appl Phys Lett 68:3820–3822

Di Nunzio S, Vitale Brovarone C, Spriano S, Milanese D, Verné E, Bergo V, Maina G, Spinelli P (2004) Silver containing bioactive glasses prepared by molten salt ion-exchange. J Eur Ceram Soc 24:2935–2942

Durucan C, Akkopru B (2010) Effect of calcination on microstructure and antibacterial activity of silver-containing silica coatings. J Biomed Mater Res B Appl Biomater 93(2):448–458

Ewald A, Gluckermann SK, Thull R, Gbureck U (2006) Antimicrobial titanium/silver PVD coatings on titanium. Biomed Eng Online 5:22

Ezz-Eldin FM, Mahmoud HH, Abd-Elaziz TD, El-Alaily NA (2008) Response of commercial window glass to gamma doses. Physica B 403:576–585

Ferraris M, Chiaretta D, Fokine M, Miola M, Verné E (2008) Patent Application TO2008A000098

Ferraris M, Perero S, Miola M, Ferraris S, Verné E, Morgiel J (2010a) Silver nanocluster–silica composite coatings with antibacterial properties. Mater Chem Phys 120:123–126

Ferraris M, Perero S, Miola M, Ferraris S, Gautier G, Maina G, Fucale G, Verné E (2010b) Chemical, mechanical, and antibacterial properties of silver nanocluster–silica composite coatings obtained by sputtering. Adv Eng Mater 12:B276–B282

Ferraris S, Perero S, Vernè E, Battistella E, Rimondini L, Ferraris M (2011) Surface functionalization of Ag-nanoclusters–silica composite films for biosensing. Mater Chem Phys 130:1307–1316

Hoa XD, Kirk AG, Tabrizian M (2007) Towards integrated and sensitive surface plasmon resonance biosensors: a review of recent progress. Biosens Bioelectron 23:151–160

http://www.agc-flatglass.sg/products-detail.aspx?id=32. Accessed 8 Nov 2012

http://www.agion-tech.com/. Accessed 8 Nov 2012

http://srdata.nist.gov/xps/selEnergyType.aspx. Accessed 8 Nov 2012

Jimenez JA, Sendova M, Hartsfield T, Sendova-Vassileva M (2011) In situ optical microspectroscopy of the growth and oxidation of silver anoparticles in silica thin films on soda-lime glass. Mater Res Bull 46:158–165 and references therein

Kawashita M, Tsuneyama S, Miyaji F, Kokubo T, Kozuka H, Yamamoto K (2000) Antibacterial silver-containing silica glass prepared by sol–gel method. Biomaterials 21:393–398

Kim YH, Lee DK, Cha HG, Kim CW, Kang YS (2007) Synthesis and characterization of antibacterial Ag–SiO₂ nanocomposite. Phys Chem C 111:3629–3635

Kim YH, Kim CW, Cha HG, Jo BK, Ahn GW, Hong ES, Kang YS (2008) Preparation of antibacterial silver-containing silica nanocomposite. Surf Rev Lett 15:117–122

Kramer SJ, Spadaro JA, Webster DA (1981) Antibacterial and osteoinductive properties of demineralized bone matrix treated with silver. Clin Orthop Relat Res 161:154–162

Landsdown ABG (2002) Silver I: its antibacterial properties and mechanism of action. J Wound Care 11:125–130

Le Houerou V, Sangleboeuf JC, Deriano S, Rouxel T, Duisit G (2003) Surface damage of soda-lime–silica glasses:

indentation scratch behaviour. J Non-Cryst Solids 316:54–63

Lucca DA, Herrmann K, Klopfstein MJ (2010) Nanoindentation: measuring methods and applications. CIRP Ann Manuf Technol 59:803–819

Martin TP, Kooi SE, Chang SH, Sedransk KL, Gleason KK (2007) Initiated chemical vapor deposition of antimicrobial polymer coatings. Biomaterials 28:909–915

Masuda N, Kawashita M, Kokubo T (2007) Antibacterial activity of silver-doped silica glass microspheres prepared by a sol-gel method. J Biomed Mater Res B Appl Biomater 83B:114–120

Mattei G, Battaglin G, Cattaruzza E, Maurizio C, Mazzoldi P, Sada C, Scremin BF (2007) Synthesis by co-sputtering of Au–Cu alloy nanoclusters in silica. J Non-Cryst Solids 353(5):697–702

Mennig M, Schmitt M, Schmidt H (1997) Synthesis of Ag-colloids in sol–gel derived SiO₂-coatings on glass. J Sol-Gel Sci Technol 8:1035–1042

Minati L, Speranza G, Calliari L, Micheli V, Baranov A, Fanchenko S (2008) The influence of metal naoparticles size distribution in photoelectron spectroscopy. J Phys Chem A 112:7856–7861

Minati L, Speranza G, Torrengo S (2010) Characteriazion of gold nanoparticles synthesized on carbon nanotubes film: evaluation of the size distribution by mean of X-ray photoelectron spectroscopy. Surf Sci 604:507–511

Morones JR, Elechiguerra JL, Camacho A, Holt K, Kouri JB, Ramírez JT, Yacaman MJ (2005) The bactericidal effect of silver nanoparticles. Nanotechnology 16:2346–2353

Najafi SI (1992) Introduction to glass integrated optics. Artech House, Norwood

Narayan P, Vaijapurkar SG, Senwar KR, Kumar D, Bhatnagar PK (2008) Application of commercial glasses for high gamma dose measurement using optical densitometric technique. Radiat Meas 43:1237–1241

NCCLS M2-A9 (2003) Performance standards for antimicrobial disk susceptibility tests, Approved Standard, 9th edn. NCCLS, Villanova

NCCLS M7-A6 (2003) Methods for dilution antimicrobial susceptibility tests for bacteria that grow aerobically, approved standard. 6th edn. NCCLS, Villanova

Rai M, Yadav A, Gade A (2009) Silver nanoparticles as a new generation of antimicrobials. Biotechnol Adv 27:76–83

Sangpour P, Babapour A, Akhavan O, Moshfegh AZ (2009) A comparative study of heat-treated Ag:SiO₂ nanocomposites synthesized by cosputtering and sol-gel methods. Surf Interface Anal 41:157–163

Sant SB, Gill KS, Burrell RE (2007) Nanostructure, dissolution and morphology characteristics of microcidal silver films deposited by magnetron sputtering. Acta Biomater 3:341–350

Scarso F, Decamps A (2007) PCT/EP2007/056126

Siketic Z, Bogdanoic Radovic I, Jaksic M, Natko S (2010) Time of flight elastic recoil detection analysis with a position sensitive detector. Rev Sci Instrum 81:0333051–0333055

Sondi I, Salopek-Sondi B (2004) Silver nanoparticles as antimicrobial agent: a case study on E. coli as a model for Gram-negative bacteria. J Colloid Interface 275:177–182

Sosa IO, Noguez C, Barrera R (2003) Optical properties of metal nanoparticles with arbitrary shapes. J Phys Chem B 107:6269–6275

Speranza G, Minati L, Chiasera A, Ferrari M, Righini GC, Ischia G (2009) Quantum confinement and matrix effects in silver-exchanged soda lime glass. J Phys Chem C 113:4445–4450

Tunc K, Olgun U (2006) Microbiology of public telephones. J Infect 53:140–143

Van Hyning DL (2007) U.S. Pat. No. 7,232,777

Verné E, Di Nunzio S, Bosetti M, Appendino P, Vitale Brovarone C, Maina G, Cannas M (2005) Surface characterization of silver-doped bioactive glass. Biomaterials 26:5111–5119

Verné E, Miola M, Vitale Brovarone C, Cannas M, Gatti S, Fucale G, Maina G, Massé A, Di Nunzio S (2009) Surface silver-doping of biocompatible glass to induce antibacterial properties. Part I: massive glass. J Mater Sci: Mater Med 20:733–740

Wang HB, wie QF, Wang JY, Hong JH, Zhao XY (2008) Sputter deposition of nanostructured antibacterial silver on polypropylene non-wovens. Surf Eng 24:70–74

Wertheim GK, di Cenzo SB, Younguqist SE (1983) Positive binding-energy shifts in small metallic clusters supported on poorly conducting substrates are shown to arise from the unit positive charge remaining on the cluster in the photoemission final state. Phys Rev Lett 51:2310–2313

Yang J, Wang EG (2006) Reaction of water on silica surfaces. Curr Opin Solid State Mater Sci 10:33–39